

Lasers in Manufacturing Conference 2013

## Verification of structural simulation results of metal-based additive manufacturing by means of neutron diffraction

T.A. Krol<sup>a\*</sup>, C. Seidel<sup>a</sup>, J. Schilp<sup>a</sup>, M. Hofmann<sup>b</sup>, W. Gan<sup>b</sup>, M.F. Zaeh<sup>c</sup><sup>a</sup>iwb Application Center Augsburg, Technische Universität München, 86153 Augsburg, Germany<sup>b</sup>Forschungs-Neutronenquelle Heinz Maier-Leibnitz (FRM II), Technische Universität München, 85748 Garching, Germany<sup>c</sup>Institute for Machine Tools and Industrial Management (iwb), Technische Universität München, 85748 Garching, Germany

### Abstract

Metal-based additive processes are characterized by numerous transient physical effects, which exhibit an adverse influence on the production result. Hence, various research approaches for the optimization of e. g. the structural part behavior exist for layered manufacturing. Increasingly, these approaches are based on the finite element analysis to be able to understand the complexity. Hereby it should be considered that the significance of the calculation results depends on the quality of modeling the process in the simulation environment. Based on a selected specimen, the current work demonstrates in which way the numerical accuracy of the residual stress state can be analyzed by utilizing the neutron diffraction. Thereby, different process parameter settings were examined.

© 2013 The Authors. Published by Elsevier B.V. Open access under [CC BY-NC-ND license](#).

Selection and/or peer-review under responsibility of the German Scientific Laser Society (WLT e.V.)

*Keywords:* Additive manufacturing; residual stress; neutron diffraction; finite element analysis

### 1. Motivation / State of the Art

Customized products in small quantities can be economically produced by using metal-based additive processes (cf. [1]). However, process-related residual stresses can lead to product failures during the part production at the manufacturing system [2]. A reduction of these stresses is therefore of great importance for enhancing the process stability. Hence, numerous research approaches for an experimental (cf. [3]) as well as

\* Corresponding author. Tel.: +49-821-56883-45; fax: +49-821-56883-50.

E-mail address: [toni.krol@iwb.tum.de](mailto:toni.krol@iwb.tum.de).

an analytical (cf. [4]) analysis and optimization of residual stresses are available. Also numerical solutions were used for this purpose (cf. [5]), because they exhibit a resource efficient choice for the determination of complex residual stress states within the product. The significance of the corresponding models depends on the quality of the provided simulation data (e. g. material values). However, not every physical effect can be mapped due to measurement limitations and necessary abstraction strategies for the reduction of simulation time (cf. [10]). On the basis of this fact it should be considered to compare the simulation results with corresponding experimental values. [2] pointed out, that the neutron diffraction can be used for this purpose. It should be noted that these examinations depend on the considered material (TRIP steel 1.2709) and therefore restrict the transferability of the results.

Within the described research approaches the material AlSi12 was used (cf. [6]). A renewed comparison between the simulation and experimental results was therefore performed for the investigated simulation models of [6]. These finite element approaches are enabling the calculation and the analysis of the structural part behavior. The focused target of reducing residual stresses in the manufactured part was analyzed by using the corresponding simulation models. In this context, [8] has also pointed out that the part-specific residual stress state depends on the utilized support design. These structures have to be used for the support of overhanging part areas during the production but are typically removed after the additive manufacturing process and are therefore not directly enhancing the product value. The results of [8] are also assisting the operator of the manufacturing system in choosing a support design which is reducing residual stresses and thereby is decreasing the risk of a building interruption due to cracks or deformations. The verification of simulation models concerning the predicted residual stress states of parts which are additively manufactured was performed within the described work by means of adjusting the support design and using the approaches of [8]. The comparison of the simulation and the experiments is described in section 4.

## 2. Structural simulation model of additively manufactured products

According to [6], it is required to define a suitable testing geometry for analyzing the residual stress state by means of the finite element analysis (FEA). In order to relate the following results to own previously performed investigations and therefore to obtain a comprehensive data base, the tilde geometry was again used for the experiments within this work. The numerical description of this geometry was described by [6] for the first time and is visualized by the corresponding meshed components in the following Fig. 1 (cf. also [9]).

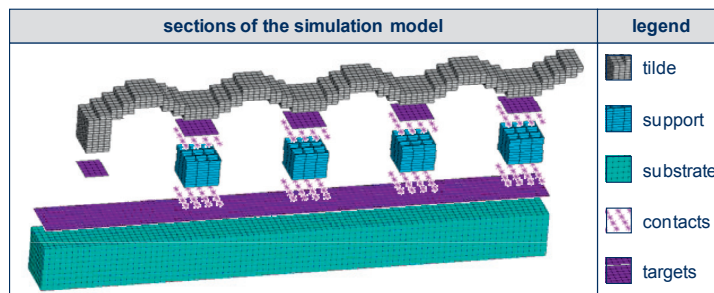


Fig. 1. Tilde specimen for the verification of residual stresses

The simulation geometry contains five single sections, which are displayed in the legend of Fig. 1. According to the corresponding CAD-geometry the tilde specimen is geometrically modeled in the thermo-physical and -mechanical simulation by means of cubic elements. The geometry contains large overhanging

areas which require support structures. These lightweight constructions are modeled within the simulation system by using so-called shell elements. This procedure enables a detailed mapping of supports in the FEA. The substrate is positioned beneath these two components. This section is used for the application of thermal (e. g. convection) and mechanical (e. g. restraint definitions) boundary conditions. Due to the resulting different meshing topologies (shape and measurement) a numerical linking of all elements for the transfer of calculated results is needed. This can be performed by using contact definitions. A contact pair is assembled with single contact elements and the corresponding target surfaces (cf. [10]).

As mentioned in section 1, the approaches of [10] are providing different abstraction and detailing levels for the process modeling within the FEA. By considering these, the simulation time can be significantly shortened, whereas the applicability of the simulation can be increased. The modeling approaches are presented in the following Fig. 2. The options for the discussed tilde specimen are highlighted with a contrasting green color.

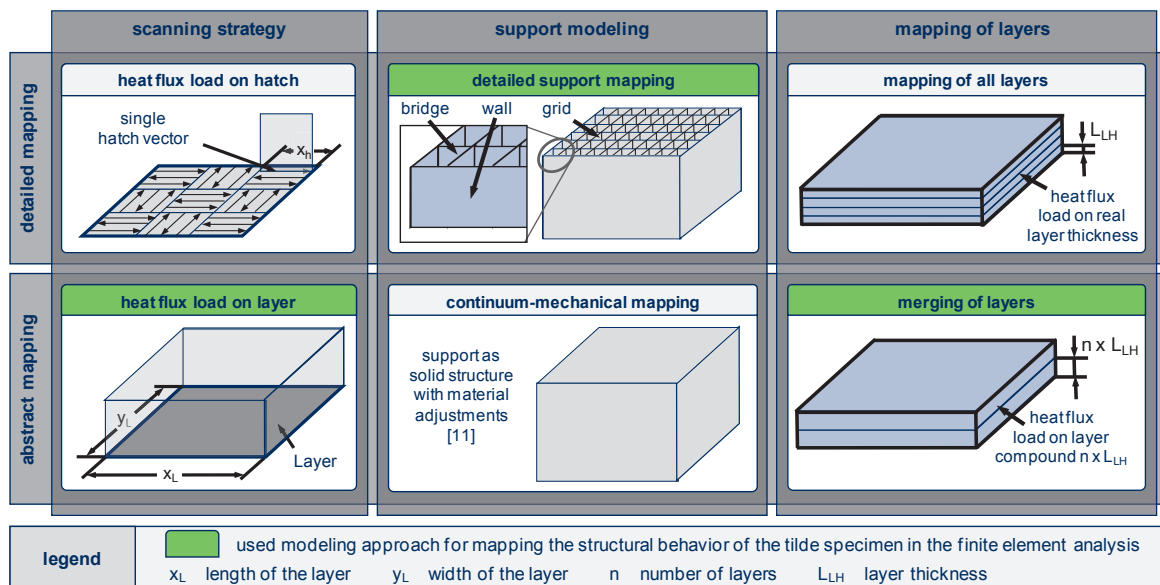


Fig. 2. Abstraction and detailing levels for additive manufacturing (in compliance with [10] and [2])

As visualized in Fig. 2, the thermal load for the simulation model was applied by utilizing a heat flux description for a whole layer. A detailed mapping of the scanning pattern was not performed in this case (cf. Fig. 2 and [10]). On the other side, the exposure strategy should be taken into account, if the solidified area of a specific layer increases. In these cases, the resulting temperature gradients from the beginning of a layer solidification (application of the heat load) until the end of the same layer's solidification (deletion of the heat load) becomes much more important. Due to the higher gradients between these two described steps, the abstraction of the exposure strategy to one calculation step would lead to higher failures in the simulation. Fig. 2 is also displaying that the options for merging of layers were used for the described application. This procedure results in a solidification of every layer compound at a single calculation step. [2] showed already in his research work that these merging options were fulfilling his defined requirements concerning the calculation accuracy when comparing the simulation and experimental results of different specimens. The modeling limit of this approach is predetermined by the shape of layers. Thus, a smaller amount of layers for

merging should be chosen, if the shapes of the layers vary a lot. Furthermore, it is also possible to map and calculate every single layer in detail.

Concerning the support design two options are available (cf. [6]). On the one hand, structures can be represented by using a continuum volume in the simulation in case the supports are shaped regularly. This approximation reduces the calculation time in the simulation. However, it is also necessary for this approach to adjust the material specifications for the consideration of the thermal and mechanical behavior of the applied support geometry. On the other hand, a geometrically detailed mapping of the support structure was used within the presented application (cf. [11]). The utilization of this approach allowed analyzing in particular the dependence of different adjusted support designs on the residual stress state (cf. chapter 1) and verifying the corresponding simulation results.

Different research works are covering approaches (also technology independent) for the reduction of the solidified support volume by means of analytical and experimental test studies (cf. [12] and [13]). In contrast, the works of [8] are also regarding structural properties for adjusting the support structure. The corresponding results for the improved support design were calculated by utilizing the finite element analysis. [8] described as a first step in their procedure how to perform a reference run by using the developed simulation models and the standardized support structures. Part areas should be selected for the following support optimization runs, which are exhibiting higher tensile stresses in the building direction than other part positions are displaying. This type of stress is often responsible for structural defects (e. g. cracks) in case they are exceeding the material specific strength properties. The corresponding part areas of the tilde geometry are the sections directly above the support structure. These are displayed in the following Fig. 3.

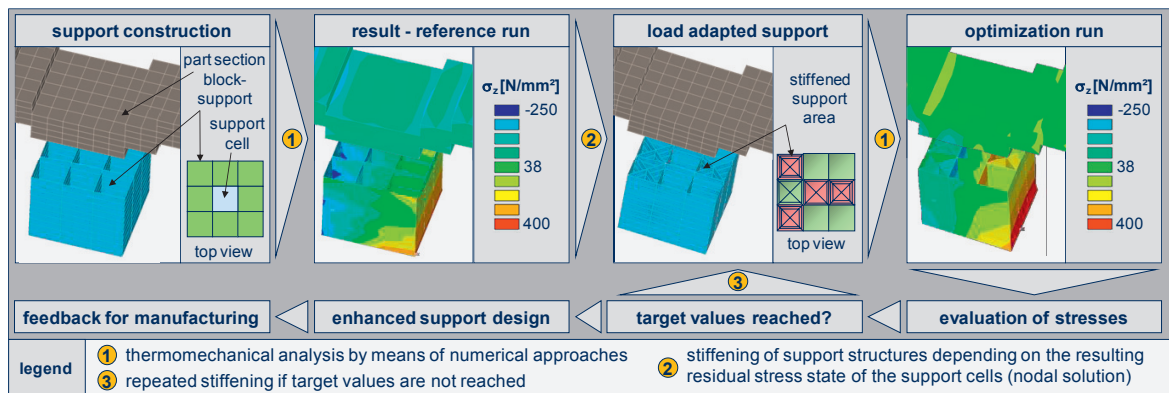


Fig. 3. Procedure for a load adapted support design by means of the resulting residual stress state (in compliance with [8])

The reference run showed that the boundary layer between the support structure and the part area tends to have a high influence on the values of the tensile stresses (cf. [8]). The resulting stresses for the corresponding nodes within the element mesh were therefore analyzed and evaluated. Hence, the risk of structural defects at these positions has been minimized (cf. point 1 in Fig. 3). Every single support cell consists of four bordering nodes (within one plane at the boundary layer) and was evaluated individually. The four values of the bordering nodes were summarized to an average stress result for every support cell. The support cell should be stiffened, if the calculated tensile stress of the currently considered support cell is above the average value for all nodal results (cf. point 2 in Fig. 3). This correlation for the load adapted adjustment of supports was already documented by [8].

As described before, the selected simulation approaches (cf. Fig. 2) were applied as a basis for the verification of the simulation results. The neutron diffraction was used to determine experimental values for a comparison.

### 3. Neutron diffraction for analyzing residual stresses in additive manufacturing

The simulation models presented in section 2 and the introduced approaches for the reduction of tensile stresses by means of adjusting the support structures have been validated. For this purpose, a comparison between the simulation and the corresponding experiment was carried out for the same process configuration. Different measurement technologies are available for obtaining experimental values of the residual stress state. The neutron diffraction enables a nondestructive examination of the resulting stresses. This technology is especially suitable for enabling a further utilization or analysis of part-specific properties. Because the parts are also used for following investigations and to finally compare these results with the previously gained residual stress values, the neutron diffraction was also used for the measurements in this case.

The STRESS-SPEC Instrument at the research reactor FRMII of the Technische Universität München was available for the measurement of residual stresses. The corresponding measurement arrangement is displayed in the following Fig. 4. The measurement gauge volume is defined by neutron absorbing slits before the specimen and a radial collimator. Neutron diffraction uses the lattice spacing as internal strain gauge. The interplanar distances ( $d_{hkl}$ ) can be extracted from the diffraction angle according to Bragg's law (cf. [7]):

$$n \times \lambda = 2 \times d \times \sin(\phi) \quad \text{Equation 1}$$

$d$  is defined as the distance of the lattice planes,  $n$  describes the diffraction order and  $\lambda$  is the adjusted wavelength (in the presented measurements  $1.55 \text{ \AA}$ ).  $\phi$  complies with the scattering angle (or bragg-angle) defined by the incoming and diffracted neutron beam. For this experiment the aluminium (311) reflection at a scattering angle of about  $2\theta_s \sim 90^\circ$  was used.

The corresponding strains were calculated using the measured interplanar distance  $d_{hkl}$  together with the  $d_{0,hkl}$  value of an unstressed reference sample. This reference specimen was manufactured by means of metal-based additive manufacturing to have the same technology-specific properties and therefore to avoid a process dependend discrepancy between the reference part and the tilde geometries. By using layered processes a completely unstressed sample cannot be produced, but it should be pointed out that a reference specimen is manufactured, which exhibits low stress states (cf. [2]). For this reason the used reference geometry for the presented measurements has the dimensions of  $5 \times 5 \times 5 \text{ mm}^3$ , was directly produced on the building plate and finally was separated from the substrate by using wire-electro discharge machining. According to [7], the strains were calculated by relating the scattering angle of the corresponding interplanar distances of the reference sample to the resulting angles of every single tilde specimen:

$$\varepsilon_{hkl} = \left( \frac{\sin(\phi_{ref})}{\sin(\phi)} \right) - 1 \quad \text{Equation 2}$$

The resulting elastic strains for the tilde specimen were measured in three perpendicular directions, namely longitudinal, transversal and normal. For the calculation of residual stresses in every single direction, the use of appropriate diffraction elastic constants was necessary [7]. A diffraction youngs' modulus of  $69.7 \text{ GPa}$  for the 311 reflection (used Millers' indices for the measurement) was used. The technically relevant stresses at a measuring point originated from overlaying of the measured strains in the main stress directions:

$$\sigma_{ij} = \frac{E}{(1+\nu)} \left[ \varepsilon_{ij} + \frac{\nu}{(1-2\nu)} (\varepsilon_{11} + \varepsilon_{22} + \varepsilon_{33}) \right] \quad \text{Equation 3}$$

In this equation,  $\nu$  describes Poisson's ratio and  $\varepsilon_{ij}$  is the previously determined strain value.  $\varepsilon_{11}$ ,  $\varepsilon_{22}$  and  $\varepsilon_{33}$  are the strains in the corresponding directions. With the application of equation 3, the calculated stresses were subsequently compared to the simulation results.

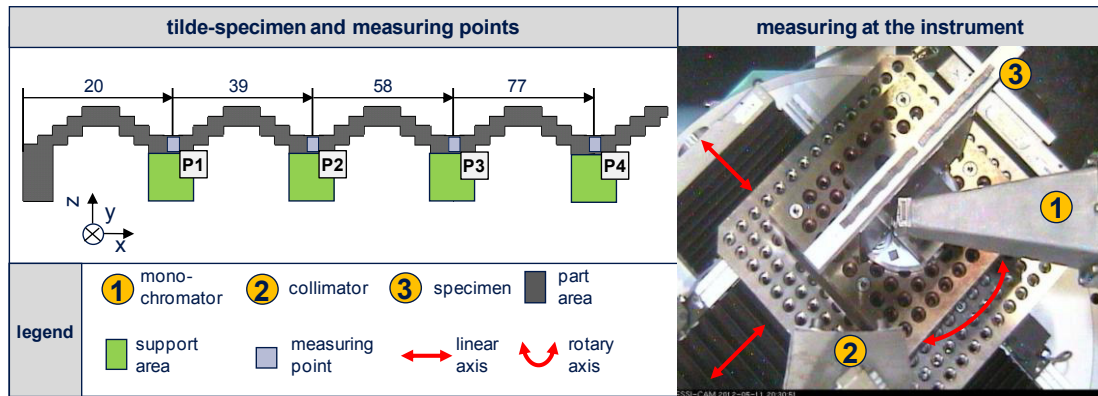


Fig. 4. Configuration for measuring residual stresses by means of neutron diffraction

Different process parameter constellations for the production of the tilde specimen were examined and the impact of these on the residual stress state was measured. The parameter sets were also considered, when parameterizing the simulation model (cf. chapter 2). The used parameter sets are listed in the following table 1.

Table 1. Selected process parameter constellations

parameter configurations	preheating	scanning velocity	support pattern
specimen 1	20 °C	standard + 20 %	block
specimen 2	20 °C	standard + 20 %	optimized
specimen 3	200 °C	standard + 20 %	block
specimen 4	200 °C	standard + 20 %	optimized
specimen 5	20 °C	standard	block
specimen 6	20 °C	standard	optimized

The used system technology for the presented experimental investigations allowed to adjust the building plate temperature. Therefore, the influence of a preheating procedure on the residual stress state was analyzed. As [2] presented in previous research works, the residual stresses can be lowered by increasing the overall process temperature. Two different temperature levels were considered in the experimental design of table 1. Furthermore, the influence of the scanning velocity was examined by means of increasing the values for the specimens 1 through 4 compared to the tilde geometries 5 and 6. Two different support structures were also varied in the experimental design of table 1. A standardized support was compared to an optimized variation. The latter one was defined by using the research results presented in section 2 and has enabled a plausibility



check for the simulation results (and also the procedure of Fig. 3) by means of a direct comparison to the experimental results. This comparison and the corresponding discussion of the results in section 4 also required the definition of measurement points for the analysis of residual stresses. Therefore and for the examination of the two selected support structures, part sections were selected, which were directly influenced from the support design concerning their residual stress state. These were the overhanging part areas of the tilde specimen, which were supported by support structures. The corresponding four measurement positions are displayed in Fig. 4 (points P1 till P4). At these positions the measurement was performed using an aperture dimension of  $2 \times 2 \text{ mm}^2$  to get sufficient measurement stability and accuracy for the neutron loading. This section was also adjusted for the simulation results to allow a value comparison between the experiment and the calculated results.

#### 4. Experimental and simulation results

The main objective of the presented approaches in chapter 2 was to reduce tensile stresses by means of adjusting the corresponding support design. In a first step the differences in the residual stress behavior of the investigated support designs (block and optimized) were examined for each equal process configuration of the preheating temperature and the scanning velocity. In the simulation as well as in the experiment the comparison of two specimens at a time was summarized within three diagrams. In the following Fig. 5, the results of the neutron diffraction experiment are displayed.

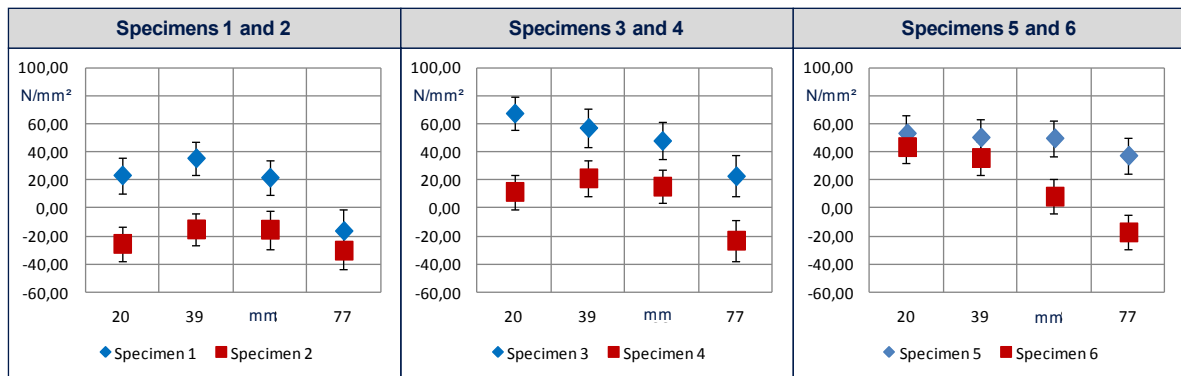


Fig. 5. Results of the residual stress measurements

It becomes clearly evident from the measurement results of Fig. 5 that the specimens which have a standardized support (tilde geometry 1, 3 and 5), tend to have higher tensile stresses compared to the specimens with the optimized support design (tilde geometry 2, 4 and 6). With comparing specimens 3 and 4, the reduction of tensile stresses is much more evident than between specimens 1 and 2. The impacts of preheating the substrate on the residual stress state can be considered for the stress progressions of specimen 1 and 2 compared to the geometries of 3 and 4. It is recognizable that for the increased process temperature (200 °C) the conventional as well as the optimized support design tends to show higher tensile stresses compared to the corresponding experiments at ambient temperature. As visualized in section 3, this behavior is contrary to the results of [2]. Due to the fact that [2] used other specimens for the analysis of residual stresses, a direct comparison between the work of [2] and the application with using the tilde geometry is not

feasible. With the improvement of the scanning velocity at 20 % (specimen 1 and 2) the tensile residual stresses can be lowered compared to specimens 5 and 6.

Fig. 6 contains the simulation results for the corresponding experimental design of table 1. These diagrams can be used for a comparison to the experimental results.

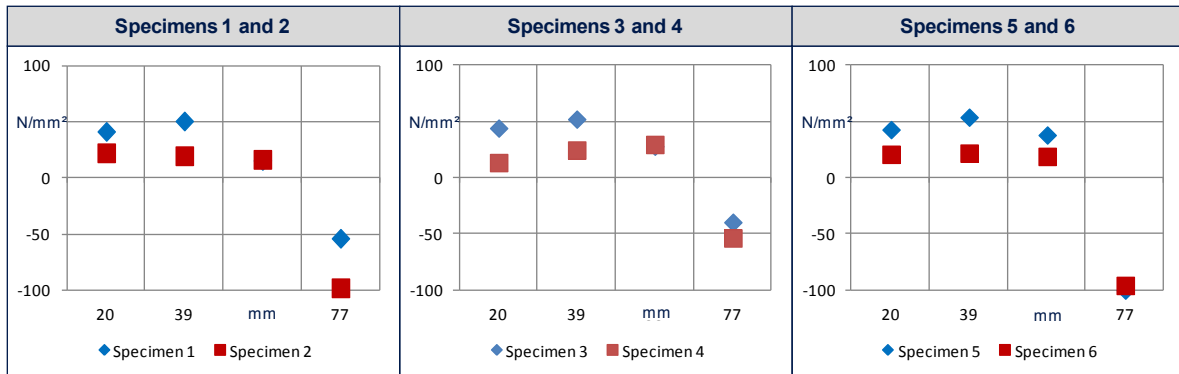


Fig. 6. Simulation results for the residual stress states

Thus, in analogy to Fig. 5, the simulation reflects the same tendencies concerning the reduction of residual stresses by means of optimizing the corresponding support structures. In contrast, the simulation values are not exhibiting influences on the residual stress state as a result of changing the parameter sets of the scanning velocity and the preheating temperature. On the one hand this can be traced back to the selected abstraction measures for modeling the process in the simulation environment (cf. Fig. 2). This behavior can be avoided, if higher detailing levels are used within the finite element models. The higher calculation time for solving the simulation problem should be kept in mind. On the other hand the quality of the measurement values depends on the used beam diaphragm during the neutron diffraction (cf. chapter 3). A smaller size would lead to lower measurement errors, but would also increase the time for receiving the same measurement stability as described before.

## 5. Summary and future perspectives

This paper describes the validation of simulation models by means of neutron diffraction. Therefore, numerical approaches for optimizing support structures were used. The application of these methods should lead to lower tensile stresses of the product. Hence, the variation of the support structure for determining their influence on the residual stress state was analyzed. An examination of different values of the scanning velocity and preheating temperature was performed. The corresponding results were displaying in the experiment and also in the simulation that a high influence of the support pattern on the residual stress state is recognizable. With the application of the optimization algorithms presented in section 2 it was shown that tensile stresses can be lowered. This results in a higher process stability (cf. [8]).

When summarizing the results of section 4 it becomes evident that the different residual stress progressions between the experiment and the simulation for the scanning velocity and the preheating temperature are traceable to the abstraction level of the used finite element models as well as the practicable gauge volume of  $2 \times 2 \times 2 \text{ mm}^3$ . With using a higher detailing level in modeling the process by means of the finite element analysis the numerical accuracy can be increased (cf. Fig. 2). By simultaneously minimizing the gauge volume



of the STRESS-SPEC-instrument, the comparability of results should be enhanced. Further investigations should determine the validity of these statements.

## Acknowledgements

This work was performed within the framework of the research project PartSUPPORT. This project is funded by the Bavarian Research Foundation. The authors thank the FESTO AG & Co. KG for the production of parts which were needed for the presented work and all further project partners for the successful cooperation.

## References

- [1] Wohlers, T. T.: Wohlers Report 2007. Fort Collins, Colorado, USA: Wohlers Associates, Inc. 2007. ISBN: 0975442937.
- [2] Branner, G.: Modellierung transients Effekte in der Struktursimulation von Schichtbauverfahren. Munich, Germany: Herbert Utz 2010. ISBN: 9783831640713.
- [3] Munsch, M.; Hallmann, S.; Emmelmann, C.: Experimental Analysis of Influence Factors on Residual Stresses in Laser Additive Manufacturing of TiAl6V4. In: Demmer, A. (ed.): Direct Digital Manufacturing Conference 2012. Berlin 2012.
- [4] Li, Y.; Chen, Y.: Beam Structure Optimization for Additive Manufacturing based on Principal Stress Lines. In: Bourell, D. L., et al. (ed.): Solid Freeform Fabrication Proceedings 2010, pp. 666–678.
- [5] Gusarov, A. V.; Pavlov, M.; Smurov, I.: Residual Stresses at Laser Surface Remelting and Additive Manufacturing. *Physics Procedia* 12 (2011) Part A, pp. 248–254.
- [6] Krol, T. A.; Zaeh, M. F.; Schilp, J.; Seidel, C.: Computational-Efficient Design of Support Structures and Material Modeling for Metal-Based Additive Manufacturing. In: CADFEM GmbH (ed.): Conference Proceedings. Grafing: CADFEM GmbH 2011.
- [7] Hutchings, M. T.; Withers, P. J.; Holden, T. M.; Lorentzen T.: Introduction to the characterization of residual stress by neutron diffraction. Boca Raton, FL, USA: Taylor & Francis Group 2005. ISBN: 0-203-40281-2.
- [8] Krol, T. A.; Záh, M. F.; Seidel, C.: OPTIMIZATION OF SUPPORTS IN METAL-BASED ADDITIVE MANUFACTURING BY MEANS OF FINITE ELEMENT MODELS. Bourell D. L.; Beaman J. J. et al. (ed.) 2012: Proceedings of the 22. Solid Freeform Fabrication Conference. University of Texas at Austin 2012.
- [9] Záh, M. F.; Krol, T. A.; Seidel, C.: Prioritisation of Process Parameters for an Efficient Optimisation of Additive Manufacturing by means of a Finite Element Method. *Procedia CIRP* 2012. (to be published).
- [10] Krol, T. A.; Westhäuser, S.; Záh, M. F.; Schilp, J.: Development of a Simulation-Based Process Chain - Strategy for Different Levels of Detail for the Preprocessing Definitions. In: Boedi, R.; Maurer, W. (ed.): ASIM 2011 - 21. Symposium Simulationstechnik. Winterthur, Schweiz. 7.-9. September 2011. ISBN: 978-3-89967-733-1.
- [11] Krol, T. A.; Zaeh, M. F.; Seidel, C.; Schilp, J.: Simulationsbasierte Optimierung der Bauteilmaßhaltigkeit bei Strahlschmelztechnologien. In: CADFEM GmbH (ed.): Conference Proceedings. Grafing: CADFEM GmbH 2012.
- [12] van Elsen, M.: Complexity of selective laser melting. PhD thesis. Katholieke Universiteit Leuven 2007.
- [13] Alexander, P.; Dutta, D.: Layered manufacturing of surfaces with open contours using localized wall thickening. *Computer-Aided Design* 32 (2000), pp. 175–189.